CODEN IEJMAT *Internet Electronic Journal of Molecular Design* **2006**, *5*, 27–48 ISSN 1538–6414
**BioChem** Press http://www.biochempress.com

**Internet Electronic Journal of Molecular Design**

January 2006, Volume 5, Number 1, Pages 27–48

Editor: Ovidiu Ivanciuc

Special issue dedicated to Professor Danail Bonchev on the occasion of the 65th birthday

# A Theoretical Study of Structures and Unimolecular Decomposition Pathways of Pyruvic Acid

Rita Kakkar, Preeti Chadha, and Deepshikha Verma

Department of Chemistry, University of Delhi, Delhi–110 007, India

Received: September 18, 2004; Revised: October 6, 2005; Accepted: November 4, 2005; Published: January 31, 2006

**Citation of the article:**

R. Kakkar, P. Chadha, and D. Verma, A Theoretical Study of Structures and Unimolecular Decomposition Pathways of Pyruvic Acid, *Internet Electron. J. Mol. Des.* **2006**, *5*, 27–48, http://www.biochempress.com.

**Internet Electronic Journal of Molecular Design**

**BioChem Press**
http://www.biochempress.com

# A Theoretical Study of Structures and Unimolecular Decomposition Pathways of Pyruvic Acid [#]

Rita Kakkar,* Preeti Chadha, and Deepshikha Verma

Department of Chemistry, University of Delhi, Delhi–110 007, India

Received: September 18, 2004; Revised: October 6, 2005; Accepted: November 4, 2005; Published: January 31, 2006

*Internet Electron. J. Mol. Des.* **2006**, *5* (1), 27–48

**Abstract**

**Motivation.** Pyruvic acid occurs naturally in the body and is the end product of the metabolism of sugar and starch. Its thermal decarboxylation reaction is important as it prevents the build–up of lactic acid in the body due to excess of pyruvic acid. However, in spite of its biochemical importance, very little is known of the structure of pyruvic acid and its decarboxylation reactions, as well as its enzymatic pathways. It was therefore considered necessary to carry out a thorough study of its reactions using a semiempirical method to test the validity of the approach, so that it could be used for studying the enzymatic pathways of pyruvic acid.

**Method.** The PM3 method was used for these calculations. Equilibrium geometries of all possible conformers and tautomers of pyruvic acid were calculated, and the geometries and calculated vibrational spectra compared with experimental data. Various decarboxylation reactions were explored and their final products discussed.

**Results.** The keto form of pyruvic acid is the most important tautomer on the potential energy surface. The lowest energy decarboxylation pathway involves the formation of hydroxyethylidene, which then isomerizes to the more stable acetaldehyde.

**Conclusions.** The results from these calculations are in agreement with those from accurate *ab initio* calculations, as well as experimental results, and this method may be profitably used for calculations of the enzymatic pathways of pyruvic acid, for which *ab initio* results are difficult owing to the large amount of computer time required.

**Keywords.** Pyruvic acid; PM3; decarboxylation; hydroxyethylidene.

## 1 INTRODUCTION

Pyruvic acid, $CH_3COCOOH$, is the traditional name for 2–oxopropanoic acid, a colorless liquid. It plays a fundamental role in biological systems [1,2]. It occurs naturally in the body and is an end product of the metabolism of sugar or starch. Its anion, pyruvate ($CH_3COCOO^-$), is also an important intermediate compound in the carbohydrate metabolism of living organisms, and is the product of glycolysis and a precursor for the Krebs cycle.

Several kinetic studies on the decomposition of pyruvic acid have been reported in the literature.

---

[#] Dedicated on the occasion of the 65th birthday to Danail Bonchev.

* Correspondence author; phone: 91–011–2766–6313; E–mail: rita_kakkar@vsnl.com.

The decarboxylation reaction has been studied experimentally by both thermal and photodissociation methods [3–6], but there is some confusion amongst results from these experiments and also from theoretical calculations.

In view of the biological importance of pyruvic acid and the conflicting results from experiments on decarboxylation, we have here carried out a theoretical investigation of this molecule and its isomers and some of their reactions using semiempirical molecular orbital theory. The preferred conformations of the pyruvic acid molecule, as well as its enol tautomer, were first determined. The vibrational spectra of the conformers were compared with the experimental spectra to confirm the most stable isomers. We then studied the decarboxylation pathways via three channels, leading, respectively, to acetaldehyde, hydroxyethylidene and vinyl alcohol. The interconversion of these three molecules was then investigated.

Although semiempirical methods overestimate the barriers to 1,2–hydrogen shifts, they do give reasonably accurate descriptions of chemical reactions. The availability of theoretical results at various degrees of sophistication and experimental data of activation energies makes pyruvic acid a convenient molecule to study, as the semiempirical calculations can be compared with other results to give an idea of their relative accuracy.

Of the semiempirical methods, the PM3 method is considered most reliable. Accordingly, we have used this method in the present calculations. The conclusions based on these calculations should pave the way for further calculations of the enzymatic pathways involving pyruvic acid that we propose to perform subsequently, and which are not possible to study with *ab initio* methods because of the large size of the systems involved.

## 2 COMPUTATIONAL DETAILS

In the present study, quantum mechanical calculations at the semiempirical PM3 [7–9] SCF levels within the framework of the MOPAC 7.0 program [9–11] were used to estimate the relative conformational stabilities and the harmonic vibrational frequencies. The molecular geometries were fully optimized with respect to the energy without any conformational or symmetry restrictions. In the MOPAC calculations, the keywords PRECISE and GNORM = 0.01 were used in all geometry optimizations. This ensured that, in most cases, a mean gradient value lower than 0.01 kcal $mol^{-1}$ $Å^{-1}$ was achieved. The calculated frequencies were used to confirm all stationary point structures as equilibrium structures or transition states. All transition states were characterized by the existence of only one imaginary vibrational frequency for motion along the reaction coordinate. Furthermore, IRC calculations were performed to confirm that the predicted transition state structures connect the relevant reactants and products.

# 3 RESULTS AND DISCUSSION

## 3.1 Relative Energy of Conformers

The pyruvic acid molecule is interesting since it can assume different conformations due to intramolecular rotation along the single C–C and C–O bonds, as well as exhibit different tautomers. Previous *ab initio* molecular orbital calculations on monomeric pyruvic acid [12–15] predicted the existence of four conformers, all exhibiting a planar heavy–atom framework with two methyl hydrogens symmetrically situated with respect to the molecular plane (Figure 1). In this work, we follow the nomenclature used for pyruvic acid conformers [12,14], which named conformers according to the $C_{methyl}$–$C_{keto}$–$C_{acid}$–$O_{hydroxyl}$ and $C_{keto}$–$C_{acid}$–O–H angles. The upper–case letter (*C*, cis; *T*, trans) refers to the former angle; the lower–case letter (*c* or *t*) refers to the latter.

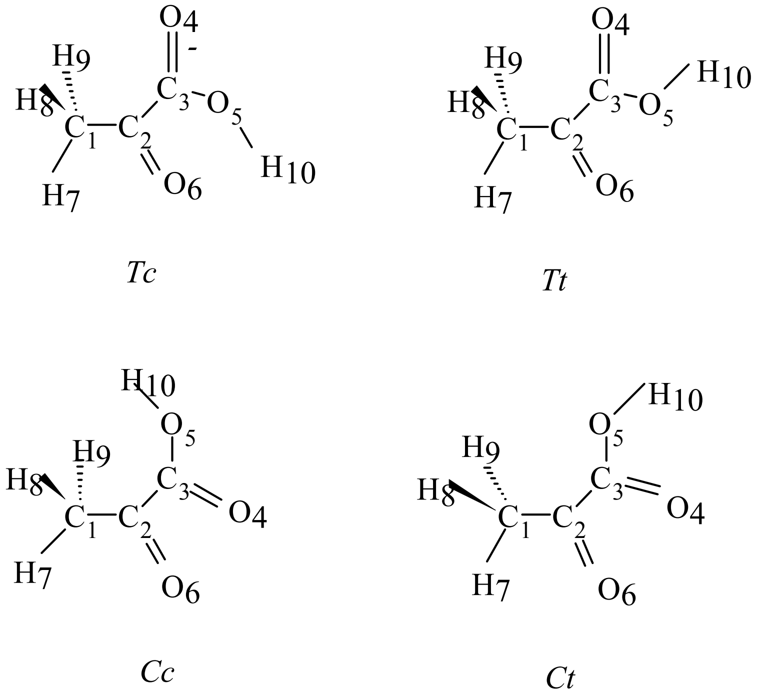

*Tc* *Tt*

*Cc* *Ct*

**Figure 1.** Conformers of pyruvic acid and atom numbering scheme.

Conformer *Tc* was found to be the lowest energy structure [12–18]. *Ct* and *Tt* species were predicted to have slightly higher energies than *Tc* (within the range 0.5 – 3 kcal/mol, depending on the level of calculation [12]). This small energy difference implies that conformers *Tt* and *Ct*, along with *Tc*, could be present in the gas–phase pyruvic acid in noticeable amounts. The fourth possible conformer, *Cc*, was predicted to have a much higher energy (from 10.7 to 12.8 kcal/mol above *Tc* [12]).

Theoretical studies [14,16–18] also analyzed in detail the exact equilibrium arrangement of the methyl group in pyruvic acid. As found for other molecules bearing a methyl group adjacent to a carbonyl (*e.g.*, acetic and thioacetic acids, acetone, acetaldehyde [19,20]), it is now well established that, in pyruvic acid, the methyl group assumes a conformation where one of the hydrogen atoms is *syn* periplanar with respect to the carbonyl oxygen [14,15]. The higher stability of this conformer is due to more favorable $\pi(CH_3) \rightarrow \pi^*(C{=}O)$ group orbital interactions and hyperconjugation through the σ bond system [18,19].

Several microwave studies of gaseous pyruvic acid have been reported [21–23]. As in the theoretical predictions, the main conclusion from these studies is that the most stable conformation is *Tc*. No other conformers have been experimentally found by this method. Reva *et al.* [14] investigated the molecular structure of pyruvic acid by matrix isolation FTIR spectroscopy, density functional theory (DFT), and *ab initio* calculations. They used the calculated harmonic frequencies and IR intensities to assist the assignment of the observed bands to the different forms. They found two conformers, both of which exhibit a planar framework with the carbonyl bonds in a *trans* arrangement, but differing in the orientation of the hydroxyl hydrogen, *i.e.*, the *Tt* and *Tc* forms. Similar results were found by Yang *et al.* [15] from their theoretical B3LYP/6–311++G(3df,3pd) calculations.

**Table 1.** Optimized geometrical parameters (see Figure 1; Å and degrees), observed and theoretical rotational constants (*A*, *B*, *C*, $cm^{-1}$), dipole moment (μ, Debye) and heat of formation ($\Delta H_f$, kcal/mol) of the pyruvic acid conformer, *Tc*.

| | PM3 | DFT [a] | MP2[a] | Expt. [b,c] |
|---|---|---|---|---|
| $C_2C_1$ | 1.495 | 1.492 | 1.499 | 1.486 |
| $C_3C_2$ | 1.536 | 1.552 | 1.545 | 1.523 |
| $O_4C_3$ | 1.212 | 1.209 | 1.218 | 1.215 |
| $O_5C_3$ | 1.346 | 1.332 | 1.347 | 1.328 |
| $O_6C_2$ | 1.214 | 1.198 | 1.233 | 1.231 |
| $H_7C_1$ | 1.098 | 1.086 | 1.096 | 1.074 |
| $H_8C_1$ | 1.099 | 1.091 | 1.101 | 1.106 |
| $H_{10}O_5$ | 0.950 | 0.974 | 0.980 | 0.983 |
| $C_3C_2C_1$ | 116.3 | 117.0 | 117.0 | 118.6 |
| $O_4C_3C_2$ | 126.4 | 125.3 | 123.0 | 122.0 |
| $O_5C_3C_2$ | 122.2 | 112.7 | 113.0 | 114.5 |
| $O_6C_2C_1$ | 123.9 | 123.1 | 125.2 | 125.0 |
| $H_7C_1C_2$ | 112.7 | 110.1 | 109.8 | 110.7 |
| $H_8C_1C_2$ | 110.3 | 109.6 | 109.2 | 109.0 |
| $H_9C_1C_2$ | 110.3 | 109.6 | 109.2 | 109.0 |
| $H_{10}O_5C_3$ | 111.1 | 107.1 | 105.6 | 105.2 |
| $O_4C_3C_2C_1$ | –3.3 | 0.0 | 0.0 | |
| $O_5C_3C_2C_1$ | 176.7 | 180.0 | 180.0 | |
| $O_6C_2C_1C_3$ | 180.0 | 180.0 | 180.0 | |
| $H_7C_1C_2C_3$ | –179.9 | 180.0 | 180.0 | |
| $H_8C_1C_2O_6$ | 120.9 | 122.0 | 121.9 | |
| $H_9C_1C_2O_6$ | –120.7 | –122.0 | –121.9 | |
| $H_{10}O_5C_3O_2$ | 0.7 | 0.0 | 0.0 | |
| A | 0.194 | – | 0.181 | 0.185 |
| B | 0.110 | – | 0.119 | 0.120 |
| C | 0.071 | – | 0.073 | 0.074 |
| μ | 2.19 | 2.38 | 2.63 | 2.30 |
| $\Delta H_f$ | –128.7 | | | |

[a] Calculated geometry from ref. [15]
[b] Experimental geometry from ref. [22]
[c] Experimental rotational constants and dipole moments from ref. [21]

**Table 2.** Optimized geometrical parameters (see Figure 1; Å and degrees), theoretical rotational constants (*A*, *B*, *C*, $cm^{-1}$), dipole moments (μ, Debye) and heats of formation ($\Delta H_f$, kcal/mol) of the pyruvic acid conformers, *Tt* and *Ct*.

| | *Tt* | | *Ct* | |
|---|---|---|---|---|
| | PM3 | DFT [a] | PM3 | DFT[a] |
| $C_2C_1$ | 1.500 | 1.501 | 1.499 | 1.503 |
| $C_3C_2$ | 1.532 | 1.551 | 1.526 | 1.558 |
| $O_4C_3$ | 1.217 | 1.201 | 1.215 | 1.199 |
| $O_5C_3$ | 1.346 | 1.336 | 1.349 | 1.351 |
| $O_6C_2$ | 1.210 | 1.203 | 1.209 | 1.194 |
| $H_7C_1$ | 1.098 | 1.086 | 1.098 | 1.086 |
| $H_8C_1$ | 1.099 | 1.091 | 1.098 | 1.091 |
| $H_9C_1$ | 1.099 | 1.091 | 1.098 | 1.091 |
| $H_{10}O_5$ | 0.953 | 0.969 | 0.953 | 0.969 |
| $C_3C_2C_1$ | 114.9 | 114.7 | 114.6 | 117.9 |
| $O_4C_3C_2$ | 127.4 | 124.9 | 128.0 | 124.3 |
| $O_5C_3C_2$ | 116.4 | 112.6 | 114.6 | 111.7 |
| $O_6C_2C_1$ | 123.6 | 122.8 | 124.7 | 124.2 |
| $H_7C_1C_2$ | 112.5 | 109.5 | 112.5 | 109.4 |
| $H_8C_1C_2$ | 110.5 | 110.0 | 110.5 | 110.2 |
| $H_9C_1C_2$ | 110.5 | 110.0 | 110.3 | 110.2 |
| $H_{10}O_5C_3$ | 110.2 | 107.5 | 110.5 | 107.5 |
| $O_4C_3C_2C_1$ | 0.1 | 0.0 | 85.5 | 0.0 |
| $O_5C_3C_2C_1$ | 180.0 | 180.0 | –93.4 | 180.0 |
| $O_6C_2C_1C_3$ | 180.0 | 180.0 | 179.2 | 180.0 |
| $H_7C_1C_2C_3$ | –179.9 | 180.0 | –178.2 | 180.0 |
| $H_8C_1C_2O_6$ | 120.7 | 121.7 | 121.6 | 121.4 |
| $H_9C_1C_2O_6$ | –120.6 | –121.7 | –119.4 | –121.4 |
| $H_{10}O_5C_3C_2$ | 180.0 | 180.0 | –178.7 | 180.0 |
| A | 0.194 | – | 0.189 | – |
| B | 0.110 | – | 0.090 | – |
| C | 0.071 | – | 0.086 | – |
| μ | 1.01 | 1.27 | 2.53 | 4.06 |
| $\Delta H_f$ | –128.6 | | –130.7 | |

[a] From ref. [15]

In the present work, all four pyruvic acid conformers (Figure 1) were investigated, but the PM3 calculations failed to locate conformer *Cc*, unless the geometry was constrained to the planar structure. Unconstrained geometry optimization converged to the conformer *Tc*. The same tendency was observed in *ab initio* calculations at the HF and MP2 levels with basis sets augmented with diffuse functions. Even the *Ct* conformer optimized to a nonplanar structure, which is lower in energy than the planar structure by 1.5 kcal/mol. The heats of formation of the conformers *Tc*, *Tt* and *Ct* are, respectively, –128.7, –128.6 and –130.7 kcal/mol. The calculated energy order is contrary to results of high–level calculations, which consistently predict the *Tc* conformer to be lowest in energy, followed by *Tt*. However, the calculated difference in energy is small. PM3 calculations also predict a nonplanar structure for the *Ct* conformer with the two carbonyl groups almost perpendicular to each other (see Table 2). In fact, the structures for the two conformers (*Ct* and *Cc*), obtained by energy minimization, keeping the geometries constrained in plane, have small imaginary vibrational frequencies, indicating that they are not minima of the potential energy surface.

Tables 1 and 2 present the optimized geometries of the three conformational states (*Tc*, *Tt* and *Ct*) of pyruvic acid calculated at the PM3 level of theory, their predicted rotational constants and dipole moments. Previously reported [21,22] experimental data for the most stable *Tc* conformer are also included in Table 1 for comparison. Good agreement can be seen with the previously calculated and experimental geometries. The *Ct* form is nonplanar.

The pyruvic acid molecule is stabilized by hydrogen bonding in the condensed phase [24]. Localized orbital studies of hydrogen bonding on the pyruvic acid molecule [25], however, revealed that the intramolecular hydrogen bonding in the *Tc* isomer of pyruvic acid is weak due to geometric restrictions on the $O_6$–$H_{10}$–$O_5$ bond angle. This explains the negligible stabilization of *Tc* relative to *Tt*.

## 3.2 Vibrational Spectra

Recently, it has been proved unequivocally [14,15] that, besides the more stable *Tc* conformer, the *Tt* conformer is also present in equilibrium. Tables 3 and 4 compare the calculated PM3 vibrational frequencies with the experimental frequencies [14] and those calculated by other methods [14,15]. Reasonable agreement with the experimental frequencies can be seen except for the O–H stretching frequency, which is overestimated. It may be noted that PM3 does not overestimate vibrational frequencies like other theoretical methods, the only exception being the O–H stretch, which needs to be scaled down by about 10%.

**Table 3.** Calculated, experimental, DFT and *ab initio* harmonic frequencies (ν, $cm^{-1}$) of the pyruvic acid conformer *Tc*.

| PM3 | Expt. [a] | DFT [b] | MP2 [a] |
|---|---|---|---|
| 3871 | 3432 | 3564 | 3477 |
| 3173 | 3032 | 3094 | 3085 |
| 3089 | | | 3037 |
| 3074 | 2936 | | 2955 |
| 1987 | 1800 | 1807 | 1791 |
| 1981 | 1728 | 1749 | 1715 |
| 1440 | 1424 | 1430 | 1439 |
| 1393 | 1408 | 1427 | 1431 |
| 1378 | 1385 | 1374 | 1397 |
| 1367 | 1355 | 1349 | 1357 |
| 1316 | 1214 | 1218 | 1245 |
| 1217 | 1137 | 1133 | 1139 |
| 992 | 1018 | | 1015 |
| 992 | 968 | 981 | 969 |
| 801 | 788 | 766 | 762 |
| 701 | 762 | 742 | 730 |
| 571 | 664 | 704 | 686 |
| 505 | 604 | 610 | 596 |
| 461 | 535 | 525 | 521 |
| 394 | 395 | | 386 |
| 384 | 388 | 391 | 384 |
| 245 | 258 | 253 | 246 |
| | 134 | | 135 |
| 94 | 90 | 90 | 94 |

[a] From ref. [14]
[b] From ref. [15]

**Table 4.** Calculated, experimental, DFT and *ab initio* harmonic frequencies (ν, $cm^{-1}$) of the pyruvic acid conformer *Tt*.

| PM3 | Expt. [a] | DFT [b] | MP2 [a] |
|---|---|---|---|
| 3844 | 3556 | 3674 | 3582 |
| 3175 | | 3093 | 3083 |
| 3089 | | 3037 | 3037 |
| 3078 | 2936 | | 2954 |
| 1990 | 1764 | 1778 | 1756 |
| 1972 | 1751 | 1765 | 1730 |
| 1453 | | 1433 | 1442 |
| 1395 | | 1430 | 1432 |
| 1382 | | 1370 | 1397 |
| 1369 | | 1347 | 1355 |
| 1249 | | 1194 | 1221 |
| 1205 | 1119 | 1118 | 1124 |
| 997 | | 1042 | 1015 |
| 994 | 962 | 971 | 963 |
| 794 | | 739 | 741 |
| 697 | 723 | 736 | 714 |
| 539 | 588 | 624 | 627 |
| 538 | 592 | 597 | 582 |
| 482 | | 514 | 511 |
| 396 | | | 383 |
| 367 | | | 375 |
| 239 | | 249 | 243 |
| 99 | | | 143 |
| | 124 | 32 | 41 |

[a] From ref. [14]
[b] From ref. [15]

## 3.3 Other Tautomers

### 3.3.1 Enol form

We also considered the enol form of pyruvic acid. This form is important, as the direct decarboxylation to vinyl alcohol would involve this tautomer. Several conformers of this tautomer are possible, too, and these are depicted in Figure 2. PM3 calculations suggest that the preferred conformer is the (*h*) conformer, but the differences in energy are extremely small. This is found to be less stable than the *Tc* form by 11 kcal/mol. This value is in agreement with the HF/6–31G** value of 12 kcal/mol [26].

The heats of formation of the eight conformers, given in Figure 2, indicate no special preference for any form. In fact, conformer (*f*) is the one involved in the isomerization to vinyl alcohol and this is only slightly less stable than the least energy conformer, (*h*). Both the (*c*) and (*g*) forms, particularly the latter, optimize to structures in which the COOH group is perpendicular to the CCC plane. The calculated vibrational frequencies for the enol forms reveal that, in the case of the (*b*) conformer, one of the vibrational frequencies is imaginary (110 $cm^{-1}$), indicating that this is not a stable minimum of the potential energy surface. The close proximity of hydrogens, $H_9$ and $H_{10}$, is responsible for the low stability of this conformer. In (*e*) and (*g*), too, the two hydrogens, $H_7$ and $H_9$, are *syn* to each other, but the latter structure is nonplanar, and the two distances are 2.369 Å and

2.377 Å, respectively, compared to 1.815 Å for (*b*).

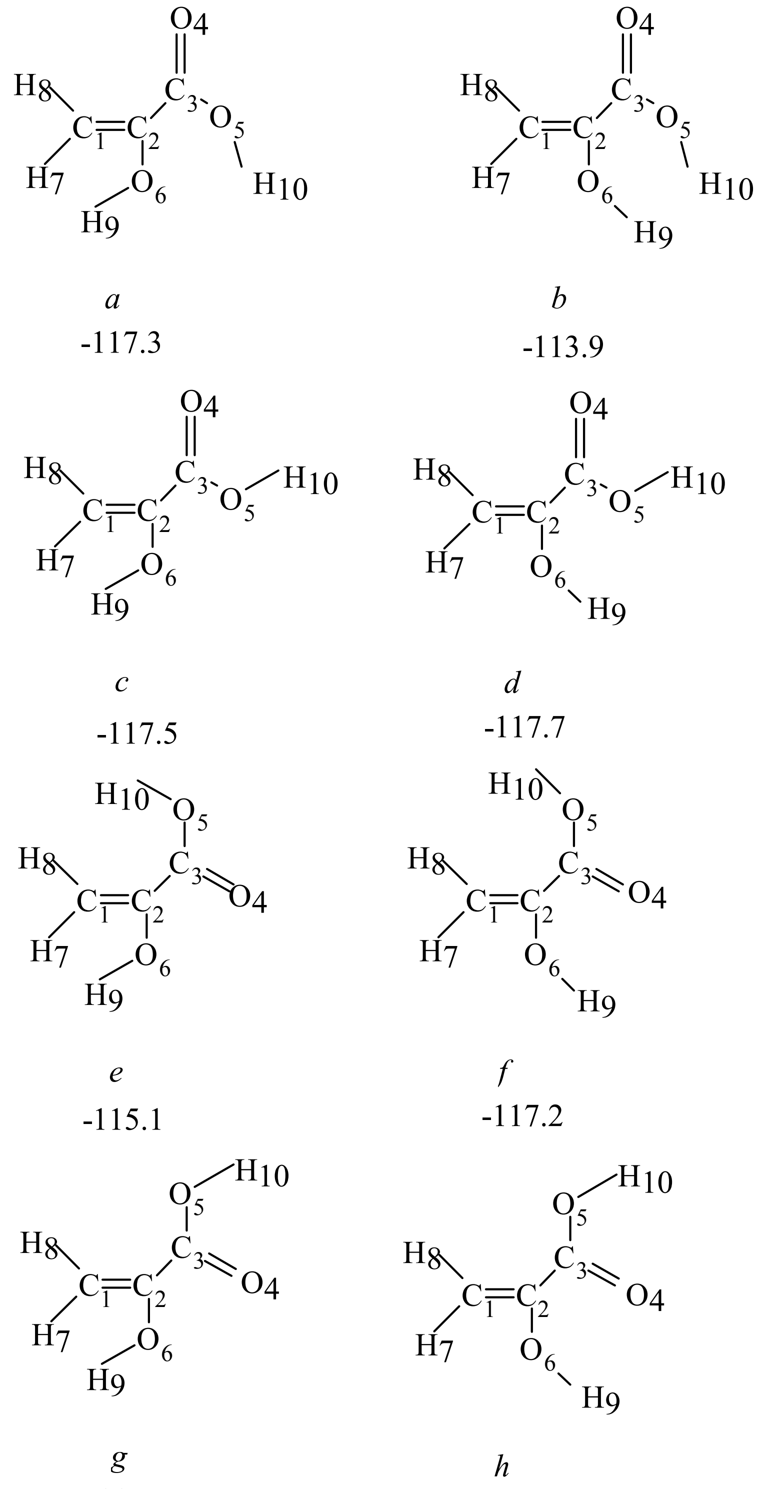

*a*
-117.3

*b*
-113.9

*c*
-117.5

*d*
-117.7

*e*
-115.1

*f*
-117.2

*g*
-117.5

*h*
-118.3

**Figure 2.** Conformers of the enol form and their heats of formation in kcal/mol.

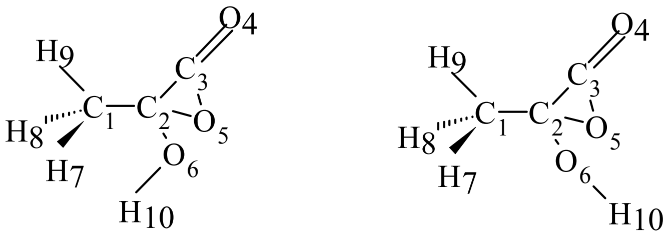

*a* *b*

**Figure 3.** Conformers of the lactone forms.

**Table 5.** Optimized geometrical parameters (see Figure 3; Å and degrees), theoretical rotational constants (*A*, *B*, *C*, cm$^{-1}$), dipole moments (μ, Debye) and heats of formation ($\Delta H_f$, kcal/mol) of the (*a*) and (*b*) lactone forms.

| | Lactone | | |
|---|---|---|---|
| | (*a*) | (*b*) | 6–311G**[a](a) |
| $C_2C_1$ | 1.506 | 1.505 | 1.500 |
| $C_3C_2$ | 1.477 | 1.480 | 1.437 |
| $O_4C_3$ | 1.192 | 1.193 | 1.163 |
| $O_5C_3$ | 1.370 | 1.326 | 1.300 |
| $O_6C_2$ | 1.380 | 1.378 | 1.347 |
| $H_7C_1$ | 1.099 | 1.098 | 1.081 |
| $H_8C_1$ | 1.098 | 1.098 | 1.087 |
| $H_9C_1$ | 1.097 | 1.097 | 1.084 |
| $H_{10}O_6$ | 0.950 | 0.949 | 0.944 |
| $C_3C_2C_1$ | 124.0 | 123.2 | 124 |
| $O_4C_3C_2$ | 160.9 | 163.3 | 155 |
| $O_5C_3C_2$ | 63.1 | 62.7 | |
| $O_6C_2C_1$ | 117.7 | 111.5 | 117 |
| $H_7C_1C_2$ | 111.6 | 111.3 | 111 |
| $H_8C_1C_2$ | 110.1 | 110.4 | 110 |
| $H_9C_1C_2$ | 111.7 | 111.4 | 110 |
| $H_{10}O_6C_2$ | 107.3 | 109.7 | 110 |
| $O_4C_3C_2C_1$ | 75.9 | –103.7 | 84 |
| $O_5C_3C_2C_1$ | –102.0 | 75.8 | –95 |
| $O_6C_2C_1C_3$ | 159.3 | 160.1 | |
| $H_7C_1C_2C_3$ | 143.3 | 143.6 | |
| $H_8C_1C_2O_6$ | 62.4 | 63.4 | |
| $H_9C_1C_2O_6$ | –177.8 | –176.5 | |
| $H_{10}O_6C_2C_3$ | –147.8 | –28.9 | |
| A | 0.209 | 0.213 | |
| B | 0.100 | 0.099 | |
| C | 0.088 | 0.087 | |
| μ | 3.72 | 1.91 | |
| $\Delta H_f$ | –87.1 | –86.6 | |

[a] From ref. [14]

### 3.3.2 Enantiomeric lactone type isomers

Two rotamers of the lactone form were considered; these are depicted in Figure 3 and the optimized geometries are given in Table 5. Each of these contains a three member C–C–O ring. The (*a*) conformer is found to be more stable. Table 5 also gives the geometries calculated at the SCF/6–311G** level [14] for this conformer. The *ab initio* calculations [14] had also indicated that the lactone forms are stable, in spite of the strained three membered rings. The vibrational frequencies show all real values.

## 3.4 Unimolecular Decomposition

Having obtained the stable conformations of pyruvic acid and its tautomers, we investigated its thermal unimolecular decomposition. The previous sections firmly establish that pyruvic acid is the most stable tautomer, and is more stable than its enol form by at least 10 kcal/mol. The decarboxylation of pyruvic acid to acetaldehyde has an important biomedical role, as it prevents excessive production of lactic acid resulting from excess of pyruvic acid.

The assumed reaction scheme, including intermediates and sequences of possible elementary conversions, is given in Scheme I. Three channels are considered: Channel 1 leads directly to acetaldehyde through a four–center–like transition state (TS1), Channel 2 leads to hydroxyethylidene through a five–center–like transition state (TS2), and Channel 3 leads to vinyl alcohol through a four–center transition state (TS3). In the Channel 3 case, TS3 is formed from the enol form. The carbene produced from Channel 2 isomerizes to acetaldehyde through TS4 or to vinyl alcohol through TS5. In addition, acetaldehyde may directly isomerize to vinyl alcohol through another transition state, TS6.

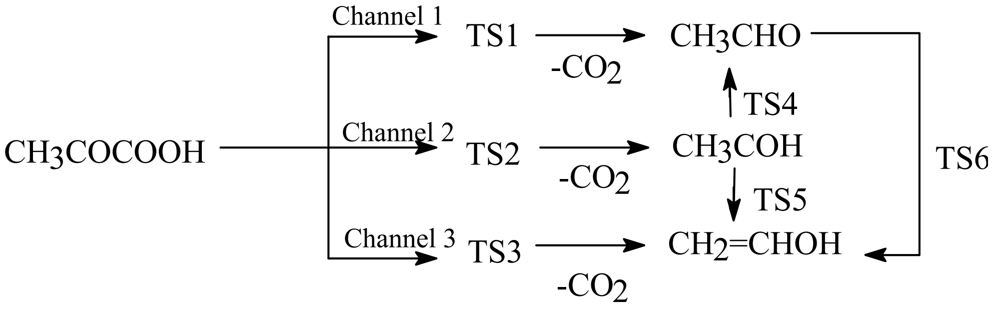

**Scheme I**

All of the fully optimized geometries of transition states were confirmed to have only one imaginary vibration corresponding to the reaction path. IRC calculations also confirmed that the transition state structures lead to the corresponding reactant and product structures. Figure 4 shows the structures and heats of formation of all the transition states involved in the decarboxylation.

It appears that the lowest potential barrier among the possible initial reactions is the path to give hydroxyethylidene and $CO_2$ through a five–center transition state (TS2). The remaining channels, which directly produce acetaldehyde and vinyl alcohol, have higher potential energy barriers. These transition states are higher than TS2 by about 28 and 35 kcal/mol, respectively, as these transition states are highly strained, having four membered rings. The low potential energy for the five–center transition state (TS2) is also not surprising if hydrogen bonding is considered. Thus, the present calculation suggests that the path to give acetaldehyde directly cannot occur. Also, Channel 3 is likewise negligible due to the high activation barrier for this channel (83.3 kcal/mol with respect to pyruvic acid). All three transition states are found to involve stretching motions along the reaction coordinate and have thus high imaginary frequencies. Note also that the imaginary frequency is higher for TS2 than for TS1 and TS3. This is because this transition state has a hydrogen simultaneously bonded to two oxygens, while the other two have a hydrogen bonded between a carbon and an oxygen. In pyruvic acid (*Tc*), the calculated O–H and C–H stretching frequencies are 3870 and 3173 cm$^{-1}$, respectively.

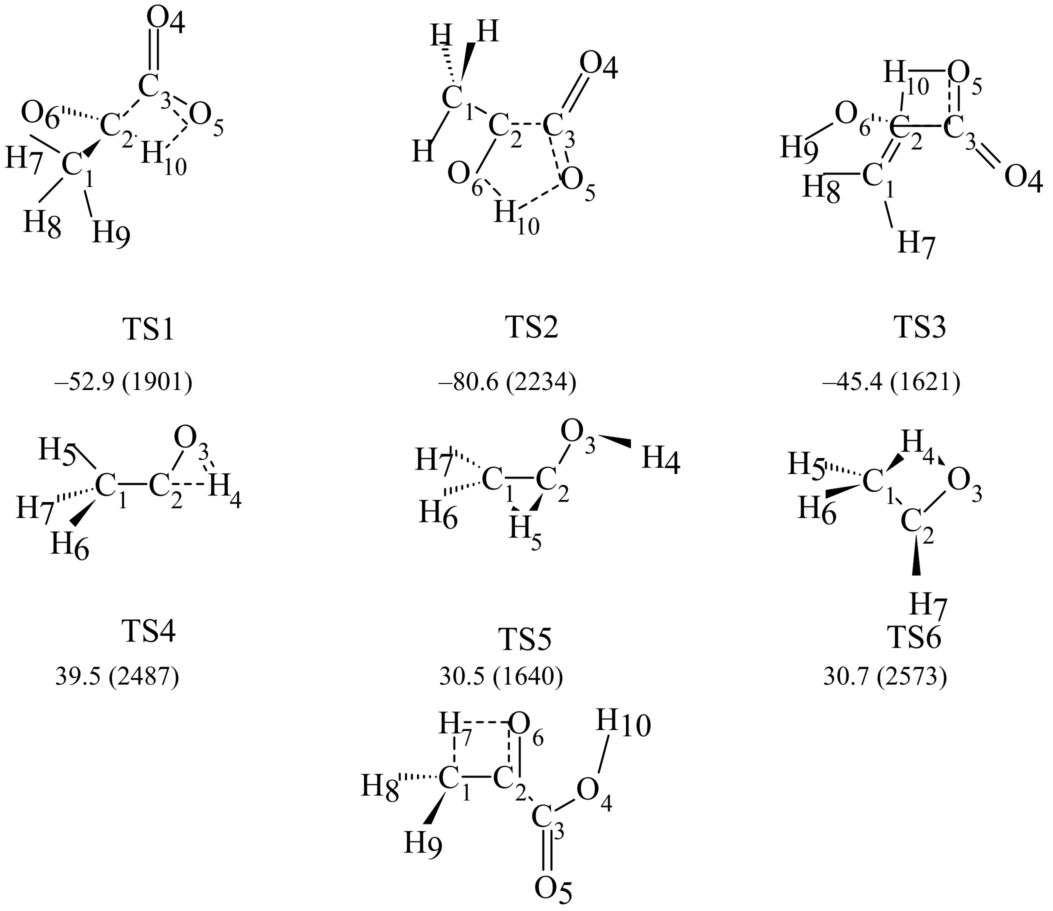

TS1
–52.9 (1901)

TS2
–80.6 (2234)

TS3
–45.4 (1621)

TS4
39.5 (2487)

TS5
30.5 (1640)

TS6
30.7 (2573)

TS7
–53.1 (2553)

**Figure 4.** Structures of transition states and their heats of formation (kcal/mol). The figures in parentheses are the corresponding imaginary frequencies (cm$^{-1}$).

Therefore, hydroxyethylidene must be an intermediate in the decarboxylation of pyruvic acid. This is in agreement with the experimental detection [26] of a product that had strong absorption bands in the vacuum–UV region. The absorption of acetaldehyde was ascertained to be negligible under the experimental conditions. The activation energy of the decomposition was found to be 40 kcal/mol, in good agreement with our calculated estimate. Hence, the unknown species produced in the decomposition is almost certainly hydroxyethylidene. Absorption bands in the vacuum–UV region have been reported for the $CH_2$ radical. It is therefore not unreasonable to expect absorption bands for hydroxyethylidene [27].

The products of the decarboxylation via Channel 1 are acetaldehyde and carbon dioxide. The reaction is slightly exothermic (Δ*H* = –0.5 kcal/mol). However, due to the high activation barrier (75.8 kcal/mol), this reaction does not seem feasible. For reaction via Channel 2, the products are hydroxyethylidene and carbon dioxide and this path has the lowest activation barrier (48.1 kcal/mol). The initial product is a hydroxyethylidene–carbon dioxide complex, in which the carbon–carbon distance of the two moieties is 2.736 Å and the OCO angle in the $CO_2$ moiety is 174.5º. Further, there is a net charge transfer of 0.016 $e^-$ from the hydroxyethylidene moiety to the $CO_2$ moiety. This complex is more stable than the separated products by 0.9 kcal/mol.

The formation of the complex is endothermic (Δ*H* = 41.3 kcal/mol). Murto *et al.* [12] also found a shallow minimum at about 3 Å in the MP2/4–31G curve for the decarboxylation of pyruvic acid. The complex is stabilized partially due to intramolecular hydrogen bonding between the OH group of *trans*–hydroxyethylidene and the nearest oxygen atom of the carbon dioxide molecule, giving rise to a five membered hydrogen–bonded ring. However, the O–H distance is calculated as 2.622 Å with the PM3 method, while *ab initio* calculations at the MP2/6–311G** level optimize to a distance of 2.007 Å [28].

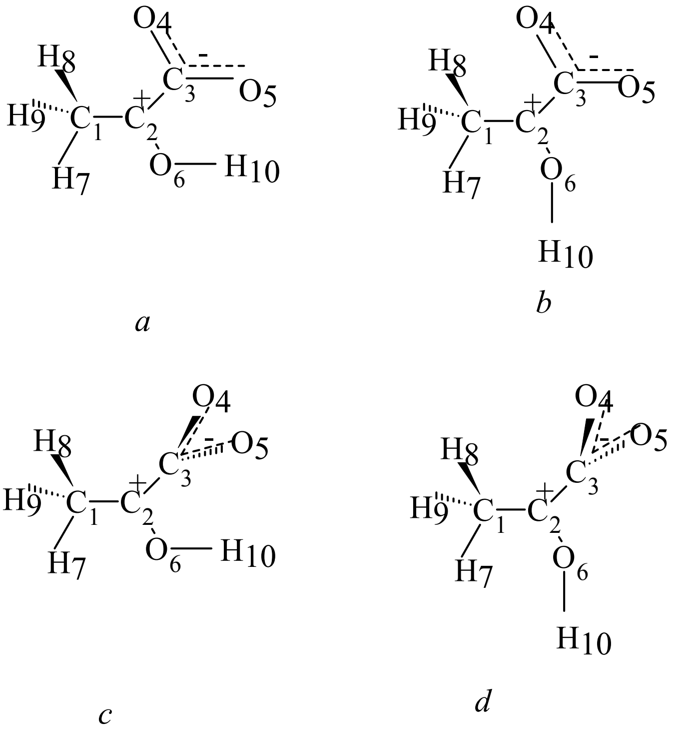

**Figure 5.** Conformers of the hydroxyethylidene–carbon dioxide complexes.

Other orientations of hydroxyethylidene–carbon dioxide complexes were also considered (Figure 5). The geometries of the carbon dioxide and hydroxyethylidene moieties in the complexes are similar to those of the isolated fragments, the difference being greatest for (*a*) due to the effect of the hydrogen bonding interaction. This can be seen by comparing these structures with the structures of hydroxyethylidene and carbon dioxide. Further, the $CO_2$ fragment in the associated systems is almost linear with an O=C=O angle in the range 174–178º. That the (*a*) complex is a true minimum was seen from the calculated vibrational frequencies. The presence of hydrogen–bonded interactions between the *trans*–hydroxyethylidene and carbon dioxide molecules in (*a*) is also indicated by the fact that the O–H stretching frequency reduces significantly (3155 $cm^{-1}$) in the (*a*) complex compared to the corresponding isolated *trans*–hydroxyethylidene structure (3884 $cm^{-1}$). Similarly, the C=O bond involved in the five membered hydrogen bonded ring has a significantly smaller vibrational frequency (2040 $cm^{-1}$) than in carbon dioxide (2386 $cm^{-1}$).

Reaction via Channel 3 involves the initial transfer of a proton from pyruvic acid to give the enol form, followed by the decarboxylation reaction giving vinyl alcohol and carbon dioxide. The initial enolization is itself a high–energy process. The transition state (TS7) is a four–centered one and is depicted in Figure 4. The activation energy required for this process (75.6 kcal/mol) is only slightly smaller than that for decarboxylation, and the latter is the rate–determining step. The overall activation energy for vinyl alcohol formation is very high, *i.e.* 83.3 kcal/mol and the preferred reaction channel is clearly Channel 2, in agreement with previous calculations.

Hence, the preferred product is hydroxyethylidene, which may subsequently undergo isomerization to the stable isomers, vinyl alcohol and acetaldehyde. The energy difference between acetaldehyde and vinyl alcohol is important as these two molecules represent the prototypical keto–enol pair. Our calculated value of 12.6 kcal/mol is in good agreement with the experimental [29] value of 10 ± 2 kcal/mol and the high–level *ab initio* [30] value of 11 kcal/mol.

### 3.4.1 Hydroxyethylidene

The experimental information on the energetics, structure, and reactivity of carbenes [31] has been reviewed. Hydroxyethylidene has been implicated as an intermediate in the photochemical decarboxylation of pyruvic acid [3] and is a likely interstellar species [32] because its more stable isomer, acetaldehyde, has been identified in the interstellar medium. A rationalization for the existence of distinct singlet *trans* and *cis* isomers is that partial C–OH double bond character forms a barrier to internal rotation of the OH group of 27.3 kcal/mol [32]. This rotational barrier has been calculated as 19.6 kcal/mol in the present calculations, and the C–OH bond order in *trans*–hydroxyethylidene is calculated as 1.451.

Energies and vibrational frequencies of singlet *trans*– and *cis*–hydroxyethylidene and also triplet hydroxyethylidene have been calculated at the SCF/3–21G–optimized geometries using several levels of theory [32]. Evanseck and Houk [33] computed MP2/6–31G*, MP2/6–311G* and MP4/6–311G** energies at the MP2/6–31G* optimized geometries for singlet *trans*– and *cis*–$CH_3COH$, while Räsänen *et al.* [34] calculated energies, geometries and vibrational frequencies for singlet *trans*– and *cis*–hydroxyethylidene using the SCF, MP2, CID, and CISD methods in conjunction with basis sets ranging from 4–31G to 6–311$^{++}$G**.

The heats of formation calculated for *trans*– and *cis*–hydroxyethylidene are –1.5 kcal/mol and –3.2 kcal/mol, respectively. The relative stability is contrary to most theoretical calculations reported in the literature [28,32–34]. Relative energies at the SCF/6–31G* [33], SCF/6–31G** [34], MP2&MP3/3–21G//SCF/3–21G [32], MP2/4–31G//SCF/4–31G [34], MP2/6–31G*//SCF/6–31G* [33], MP2/6–31G**//MP2/6–31G** [34], MP2&MP3&MP4/6–31G**//MP2/6–31G** [33], SCF/6–311G** [28], MP2/6–311G** [28], and various CID and CISD levels with 3–21G, 4–31G, and 6–31G** basis sets [32,34] have also been reported. In all cases, the *trans* conformer was found to be more stable than the *cis* conformer, and this is to be expected, since the *cis* conformer is likely to exhibit steric repulsion between the OH group and the in–plane methyl C–H bond [32], and both conformers are predicted to be planar (except for two of the methyl group hydrogen atoms).

The PM3 optimized geometries are compared with literature geometries [28,33,34] in Table 6. Calculation of the vibrational frequencies, shown in Table 7, verifies that the geometries optimized for *trans*– and *cis*–$CH_3COH$ represent true minima on their respective potential energy surfaces. The computed vibrational frequencies are in good agreement with the *ab initio* values [28], except that the latter are somewhat higher. This is because the authors had reported the unscaled vibrational frequencies. It is well known that *ab initio* methods overestimate vibrational frequencies by 10%. For the PM3 calculations on pyruvic acid, we saw that no scaling factor is required, except for the O–H frequencies, which are overestimated by 10%.

**Table 6.** Optimized geometrical parameters (Ångstroms and Degrees), theoretical rotational constants (*A*, *B*, *C*, cm$^{-1}$), dipole moments (μ, Debye) and heats of formation ($\Delta H_f$, kcal/mol) of *trans*– and *cis*–hydroxyethylidene.

| | *Trans* | | *Cis* | |
|---|---|---|---|---|
| | PM3 | *Ab initio* $^a$ | PM3 | *Ab initio* $^a$ |
| $C_2C_1$ | 1.476 | 1.500 | 1.477 | 1.502 |
| $O_3C_2$ | 1.290 | 1.317 | 1.253 | 1.303 |
| $H_4O_3$ | 0.953 | 0.964 | 0.968 | 0.981 |
| $H_5C_1$ | 1.099 | 1.096 | 1.101 | 1.106 |
| $H_6C_1$ | 1.099 | 1.095 | 1.098 | 1.094 |
| $H_7C_1$ | 1.099 | 1.095 | 1.098 | 1.094 |
| $O_3C_2C_1$ | 113.0 | 107 | 121.8 | 111 |
| $H_4O_3C_2$ | 106.9 | 106 | 118.0 | 112 |
| $H_5C_1C_2$ | 118.2 | 115 | 116.9 | 115 |
| $H_6C_1C_2$ | 107.3 | 107 | 108.0 | 108 |
| $H_7C_1C_2$ | 107.3 | 107 | 108.0 | 108 |
| $H_4O_3C_2C_1$ | 180.0 | 180 | 0.0 | 0 |
| $H_5C_1C_2O_3$ | –0.3 | 0 | –0.3 | 0 |
| $H_6C_1C_2O_3$ | 122.4 | | 122.0 | |
| $H_7C_1C_2O_3$ | –122.9 | | –122.3 | |
| A | 2.044 | | 2.051 | |
| B | 0.338 | | 0.334 | |
| C | 0.307 | | 0.304 | |
| μ | 1.07 | | 2.78 | |
| $\Delta H_f$ | –1.5 | | –3.2 | |

$^a$ From ref. [28]

**Table 7.** Calculated harmonic frequencies (ν, $\mathrm{cm}^{-1}$) for *trans*– and *cis*–hydroxyethylidene

| *Trans* | | *Cis* | |
|---|---|---|---|
| PM3 | *Ab initio* [a] | PM3 | *Ab initio* [a] |
| 167 | 43 | 172 | 102 |
| 480 | 544 | 492 | 570 |
| 652 | 789 | 711 | 764 |
| 862 | 979 | 921 | 969 |
| 915 | 1047 | 936 | 1038 |
| 1119 | 1156 | 1105 | 1159 |
| 1338 | 1420 | 1316 | 1441 |
| 1366 | 1472 | 1362 | 1474 |
| 1380 | 1512 | 1370 | 1499 |
| 1444 | 1575 | 1408 | 1561 |
| 1606 | 1586 | 1658 | 1594 |
| 3068 | 3146 | 3060 | 3079 |
| 3082 | 3216 | 3073 | 3205 |
| 3167 | 3227 | 3164 | 3231 |
| 3884 | 4136 | 3626 | 3953 |

[a] From ref. [28]

### 3.4.2 Barriers to intramolecular rearrangements

There has been considerable experimental interest in the relative magnitudes of the barriers to intramolecular rearrangements connecting acetaldehyde, vinyl alcohol and hydroxyethylidene, but agreement as to the ordering of the barriers has yet to be reached. Initial information on this point came from studies of the thermal decarboxylation of pyruvic acid. Wesdemiotis and McLafferty [27] used the technique of neutralization–reionization–mass spectrometry (NRMS) to study hydroxyethylidene. On the basis of labeling studies, these authors proposed that (*i*) the energy barrier required for the 1,2–hydrogen shift separating hydroxyethylidene from acetaldehyde should be smaller than the 1,2–hydrogen shift separating hydroxyethylidene from vinyl alcohol, and (*ii*) the transition structures associated with both these 1,2–hydrogen shifts should be lower in energy than that associated with the 1,3–hydrogen shift that directly converts vinyl alcohol to acetaldehyde.

There have been a number of *ab initio* studies of various aspects of the potential energy surface connecting the three isomers [12,32,34,35]. These predicted, among other things, that the transition structure linking hydroxyethylidene with acetaldehyde (1,2–hydrogen shift) might lie up to 25 kcal/mol above that separating vinyl alcohol from acetaldehyde (1,3–hydrogen shift), in apparent conflict with some of the conclusions from the experimental studies [3,4,27]. Smith *et al.* [30] also carried out *ab initio* calculations at the Hartree–Fock (HF) level with the 6–31G(d) and 6–31G(d,p) basis sets at the correlated level by using second order Møller–Plesset perturbation theory (MP2) with the 6–31G(d) basis set. They found that hydroxyethylidene is separated by significant barriers from its lower energy isomers, acetaldehyde and vinyl alcohol. Further, they found that the transition state connecting vinyl alcohol and acetaldehyde is lower in energy than those connecting hydroxyethylidene with the other two isomers, which also does not agree with conclusions based on experimental observations.

**Table 8.** Optimized geometrical parameters (Ångstroms and Degrees), theoretical rotational constants (*A*, *B*, *C*, $cm^{-1}$), and dipole moment (μ, Debye) of TS4.

| | PM3 | *Ab initio* [a] |
|---|---|---|
| $C_2C_1$ | 1.468 | 1.490 |
| $O_3C_2$ | 1.270 | 1.325 |
| $H_4C_2$ | 1.341 | 1.285 |
| $H_5C_1$ | 1.098 | 1.096 |
| $H_6C_1$ | 1.098 | 1.094 |
| $H_7C_1$ | 1.098 | 1.094 |
| $O_3C_2C_1$ | 122.2 | 115.1 |
| $H_4C_2C_1$ | 179.8 | |
| $H_5C_1C_2$ | 115.6 | 110.4 |
| $H_6C_1C_2$ | 108.6 | 123.6 |
| $H_7C_1C_2$ | 108.6 | 123.6 |
| $H_4C_2C_1O_3$ | 160.2 | |
| $H_5C_1C_2O_3$ | 0.6 | |
| $H_6C_1C_2O_3$ | 122.5 | |
| $H_7C_1C_2O_3$ | –121.2 | |
| A | 2.113 | |
| B | 0.328 | |
| C | 0.300 | |
| μ | 1.21 | |

[a] From ref. [30]

**Table 9.** Optimized geometrical parameters (Ångstroms and Degrees), theoretical rotational constants (*A*, *B*, *C*, $cm^{-1}$) and dipole moment (μ, Debye) of TS5.

| | PM3 | *Ab initio* [a] |
|---|---|---|
| $C_2C_1$ | 1.398 | 1.391 |
| $O_3C_2$ | 1.331 | 1.370 |
| $H_4O_3$ | 0.950 | 0.970 |
| $H_5C_1$ | 1.437 | 1.355 |
| $H_6C_1$ | 1.088 | 1.095 |
| $H_7C_1$ | 1.089 | 1.085 |
| $O_3C_2C_1$ | 117.8 | 110.7 |
| $H_4O_3C_2$ | 104.8 | 106.1 |
| $H_5C_2O_3$ | 115.9 | |
| $H_6C_1C_2$ | 117.0 | 123.9 |
| $H_7C_1C_2$ | 126.2 | 117.8 |
| $H_4O_3C_2C_1$ | –177.0 | |
| $H_5C_2O_3H_4$ | –107.0 | |
| $H_6C_1C_2O_3$ | –164.2 | |
| $H_7C_1C_2O_3$ | –4.6 | |
| A | 2.150 | |
| B | 0.342 | |
| C | 0.308 | |
| μ | 1.29 | |

[a] From ref. [30]

We have here calculated these barriers using the PM3 method. The first transformation studied here was the one yielding acetaldehyde from *trans*–hydroxyethylidene. The barrier to this transformation is calculated as 41.0 kcal/mol, which is considerably higher than the *ab initio* estimate of 28.2 kcal/mol. The transition state, TS4, has a three–center–like structure, and is depicted in Figure 4. Its optimized geometry is given in Table 8, where it is compared with the *ab initio* geometry. The transition state, TS5, connecting hydroxyethylidene to vinyl alcohol also has a three–center–like structure (see Figure 4 and Table 9) and the barrier to this rearrangement is 32.0 kcal/mol, compared to the *ab initio* [30] value of 23.4 kcal/mol. This is consistent with the fact that semiempirical methods overestimate barriers to 1,2–hydrogen shifts. The high barrier energy is in agreement with experimental results [27] that hydroxyethylidene, despite its very high energy, should be observable, since it is separated from the lower energy isomers, acetaldehyde and vinyl alcohol, by significant barriers.

The transition state, TS6, connecting acetaldehyde to vinyl alcohol through a direct 1,3–hydrogen shift, was also examined. The barrier to this shift is calculated as 74.9 kcal/mol from acetaldehyde, and this transition state has a four–center–like structure (see Figure 4 and Table 10).

**Table 10.** Optimized geometrical parameters (Ångstroms and Degrees), theoretical rotational constants (*A*, *B*, *C*, $cm^{-1}$) and dipole moment (μ, Debye) of TS6.

| | PM3 | *Ab initio* [a] |
|---|---|---|
| $C_2C_1$ | 1.408 | 1.405 |
| $O_3C_2$ | 1.286 | 1.294 |
| $H_4O_3$ | 1.357 | 1.293 |
| $H_5C_1$ | 1.095 | 1.091 |
| $H_6C_1$ | 1.084 | 1.086 |
| $H_7C_2$ | 1.090 | 1.092 |
| $O_3C_2C_1$ | 108.8 | 111.0 |
| $H_4O_3C_2$ | 82.7 | |
| $H_5C_1C_2$ | 119.2 | 112.9 |
| $H_6C_1C_2$ | 122.0 | 121.7 |
| $H_7C_2C_1$ | 130.8 | 130.6 |
| $H_4O_3C_2C_1$ | 3.6 | |
| $H_5C_1C_2O_3$ | 63.4 | 65.3 |
| $H_6C_1C_2O_3$ | –148.1 | –153.6 |
| $H_7C_2C_1H_4$ | 173.1 | |
| A | 1.530 | |
| B | 0.418 | |
| C | 0.340 | |
| μ | 1.10 | |

[a] From ref. [30]

## 4 DISCUSSION

The results obtained in the present work are summarized in Figures 6 and 7. The former displays the pathways from the keto form of pyruvic acid to vinyl alcohol and acetaldehyde, while the latter depicts the pathway to vinyl alcohol via the enol form. The latter pathway is immediately ruled out on the grounds that it involves a high–energy transition state (TS3), yielding the relatively unstable product, vinyl alcohol. Since the thermodynamically stable product is acetaldehyde, which is also the product of the enzymatic decarboxylation of pyruvic acid, we consider its formation via the two routes depicted in Figure 6. As stated previously, the direct formation of acetaldehyde via TS1 requires an activation energy of 75.8 kcal/mol. The alternate mechanism via hydroxyethylidene (TS2) and TS4 requires still higher activation energy (83.2 kcal/mol). The least energy pathway is via TS5 leading to vinyl alcohol first and then to acetaldehyde via TS6 and this has an activation energy of 73.4 kcal/mol. However, since both pathways (involving TS1 and TS6) have approximately the same barriers, both mechanisms should be operative. Experimental studies support the former mechanism, as, when O–*d*–labeled pyruvic acid is used as starting material, $CH_2DCHO$ is not observed [27], which rules out the intermediacy of vinyl alcohol.

In this discussion, we have not considered the role of solvent. Detailed effects of solvation on the relative barriers will be reported in a future communication, but some comments may be made. As stated above, the relative importance of the different pathways depends on the relative energies of TS1, TS4 and TS6. The calculated dipole moments for the three transition states are 3.80, 1.21 and 1.10 Debye, respectively, suggesting that direct decarboxylation to acetaldehyde via TS1 will be the preferred mode in aqueous solution because of the larger stabilization of the higher dipole moment transition state, in agreement with experimental results.

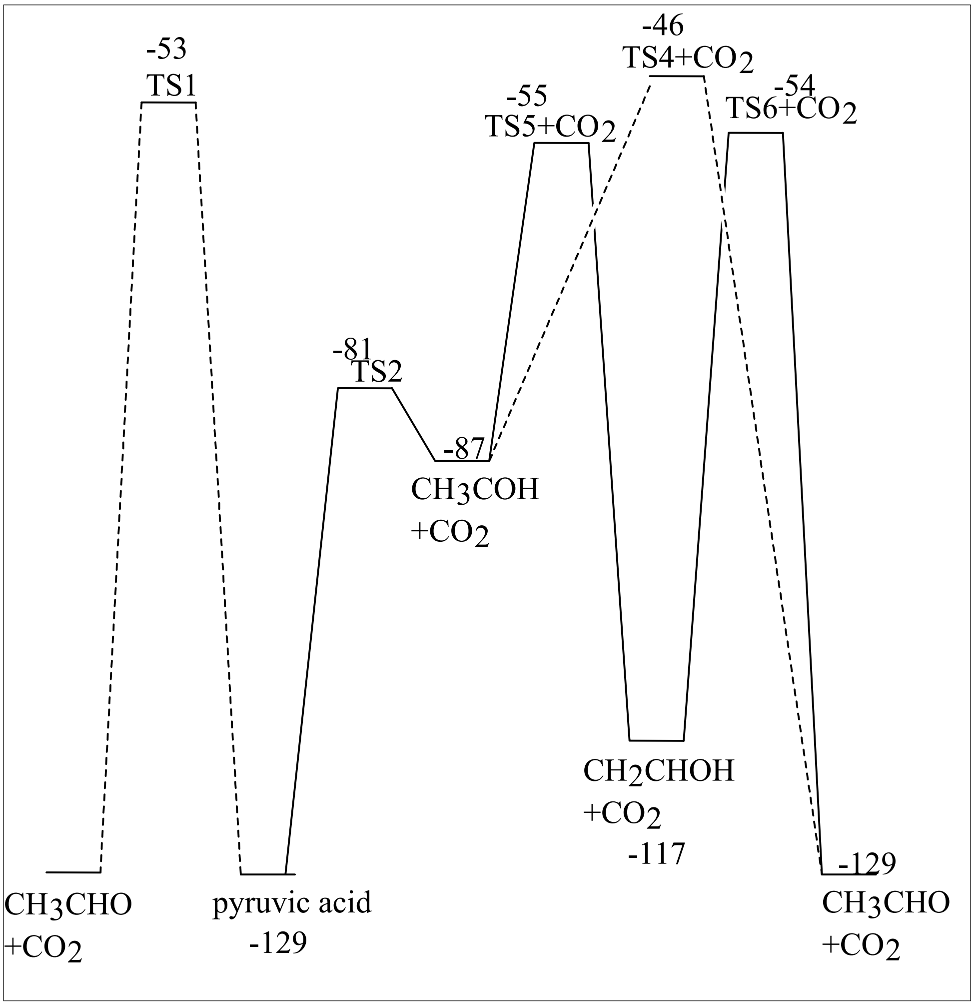

**Figure 6.** A schematic potential energy diagram (kcal/mol) decarboxylation of pyruvic acid.

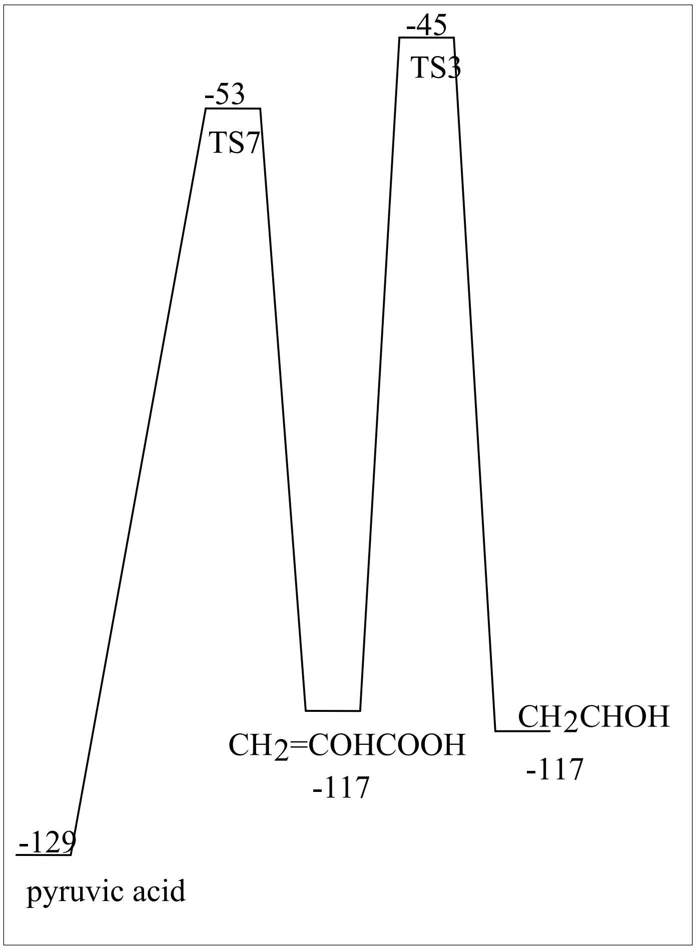

**Figure 7.** A schematic potential energy diagram (kcal/mol) for the decarboxylation of pyruvic acid to vinyl alcohol via the enol tautomer.

The calculated barriers are, however, too high for them to be directly operative in biological systems, even after making allowances for the fact that semiempirical calculations yield higher barriers for 1,2 hydrogen shift reactions. Most biochemical reactions involve relatively small energy changes. This principle is axiomatic because large energy changes cannot be utilized by the cell and will lead to disruption of cellular processes or cell death. Therefore, biochemical reactions in which a bond is broken are invariably coupled to those in which a new bond is formed, as in the steps in the respiratory chain where dioxygen is reduced in a stepwise fashion to water and ATP is generated in the various steps. In the case of pyruvate, decarboxylation occurs when it is temporarily bonded by a membrane–bound molecule called coenzyme A, which strips from pyruvate one carbon dioxide molecule, which is released as waste from the cell, as well as two electrons and hydrogen protons which are collected by NAD, reducing it to NADH + $H^+$. The new intermediate, acetyl coenzyme A, exists for only a short period of time, and then is degraded into two molecules, the original coenzyme A which is now available to bond to another pyruvate, and acetaldehyde (acetate). Acetate can either participate in the next phase of respiration, called the Krebs Tricarbolic Acid Cycle (TCA), or in alcoholic fermentation. The enzymatic pathway thus leads to energy changes in manageable amounts.

## 5 CONCLUSIONS

To sum up, the results of the present studies on the thermal decomposition of pyruvic acid, with the relatively inexpensive PM3 method, indicate that the keto form is more stable than the enol form by 11 kcal/mol, and the two tautomers are separated by a large energy barrier (76 kcal/mol). However, the predicted stability order among the various conformers of the keto structures is at variance with *ab initio* calculations, which predict the *Tc* conformer to be most stable. The calculated vibrational frequencies agree well with those calculated by *ab initio* methods and experimental determinations. Contrary to expectations, the enantiomeric lactone forms represent energy minima despite the presence of a three membered ring.

The most feasible decomposition reaction from pyruvic acid is the formation of carbon dioxide and hydroxyethylidene, which isomerizes to the thermodynamically more stable product acetaldehyde eventually. The direct decarboxylation of pyruvic acid to acetaldehyde is more expensive in terms of energy. Similarly, direct formation of the third isomer, vinyl alcohol is also not possible. However, if one considers the overall barrier to the formation of acetaldehyde, both mechanisms, i.e., direct and via hydroxyethylidene and vinyl alcohol, involve practically the same amount of activation energy (76 and 73 kcal/mol, respectively), and should be equally probable. Preliminary calculations suggest that the direct formation of acetaldehyde will be favored in aqueous media, as the involved transition state (TS1) has the highest dipole moment.

The carbene, hydroxyethylidene, is predicted to be quite stable, as it is separated by large energy barriers (> 30 kcal/mol) from its more stable isomers, acetaldehyde and vinyl alcohol. It initially forms a complex with carbon dioxide, which subsequently isomerizes to acetaldehyde and carbon dioxide.

All these conclusions are in consonance with experiment. Thus the PM3 calculations explain the experimental results satisfactorily, and may be profitably used for further work on the enzymatic pathway that we propose to undertake. However, it may be pointed out that semiempirical methods generally predict barriers, particularly for 1,2 hydrogen shifts, that are too high. More refined calculations on the energy barriers may produce results that may be significantly different from those reported here, and may alter the conclusions. Moreover, detailed effects of solvent need to be examined. Because of the biochemical importance of this reaction, we are pursuing more sophisticated calculations at the Density Functional theory level for comparison with the PM3 results, and to investigate other details of the potential energy surface, including solvent effects. The results of these calculations will be reported in a future communication, and may provide a framework for extrapolation of PM3 calculations on the enzymatic pathway of pyruvic acid decarboxylation.

**Acknowledgment**

One of the authors (P.C.) thanks the Council of Scientific and Industrial Research (CSIR), New Delhi, for a Research Fellowship.

## 5 REFERENCES

[1] A. J. L. Cooper, J. Z. Ginos, and A. Meister, Synthesis and properties of the alpha–keto acids, *Chem. Rev.* **1983**, *83*, 321–358.

[2] J. Sherman, D. Luciano, and A. J. Vander, *Human Physiology: the Mechanisms of Body Functions*, WCB McGraw–Hill, New York, 1998.

[3] R. N. Rosenfeld and B. Weiner, Energy disposal in the photofragmentation of pyruvic acid in the gas phase, *J. Am. Chem. Soc.* **1983**, *105*, 3485–3488.

[4] B. R. Weiner and R. N. Rosenfeld, Pyrolysis of pyruvic acid in the gas phase. A study of the isomerization mechanism of a hydroxycarbene intermediate, *J. Org. Chem.* **1983**. *48*, 5362–5364; and references therein.

[5] R. Taylor, The mechanism of thermal eliminations. Part XXVIII. Thermal decomposition of benzoyl formic acid, *Int. J. Chem. Kinet.*, **1991**, *23*, 247–250.

[6] J. A. O'Neill, T. G. Kreutz, and G. W. Flynn, IR diode laser study of vibrational energy distribution in $CO_2$ produced by UV eximer laser photofragmentation of pyruvic acid. *J. Chem. Phys.* **1987**, *87*, 4598–4605.

[7] J. J. P. Stewart, Optimization of parameters for semiempirical methods. 1. Method, *J. Comput. Chem.* **1989**, *10*, 209–220.

[8] J. J. P. Stewart, Optimization of parameters for semiempirical methods. 2. Applications, *J. Comput. Chem.* **1989**, *10*, 221–264.

[9] J. J. P. Stewart, MOPAC: A Semi–Empirical Molecular Orbital Program, *J. Comput.–Aided Mol. Des.* **1990**, *4*, 1–105.

[10] J. J. P. Stewart, Comments on A comparison of AM1 with the recently developed PM3 method– Reply, *J. Comput. Chem.* **1990**, *11*, 543–544.

[11] J. J. P. Stewart, MOPAC 6.0: A General Molecular Orbital Package, *Quantum. Chem. Prog. Exch. Bull.* **1990**, *10(4)*, 86.

[12] J. Murto, T. Raaska, H. Kunttu, and M. Räsänen, Conformers and vibrational spectra of pyruvic acid: an *ab initio* study, *J. Mol. Struct.: THEOCHEM* **1989**, *200*, 93–101.

[13] C. Chen and S. F. Shyu, Theoretical study of glyoxalic and pyruvic acids: rotamers and intramolecular hydrogen bonding. *J. Mol. Struct.: THEOCHEM* **2000**, *503*, 201–211.

[14] I. D. Reva, S. G. Stepanian, L. Adamowicz, and R. Fausto, Combined FTIR matrix isolation and *ab* initio studies of pyruvic acid: proof for existence of the second conformer, *J. Phys. Chem. A* **2001**, *105*, 4773–4780.

[15] X. Yang, G. Orlova, X. J. Zhou, and K. T. Leung, A DFT study on the radical, monomer and dimer of α–keto pyruvic acid: equilibrium structures and vibrational analysis of stable conformers, *Chem. Phys. Lett.* **2003**, *380*, 34–41.

[16] C. van Alsenoy, L. Schäfer, K. Siam, and J. D. Ewbank, *Ab initio* studies of structural features not easily amenable to experiment: Part 65. *Ab initio* molecular structures of glyoxylic, pyruvic, and propiolic acid, and comparison with microwave data, *J. Mol. Struct.: THEOCHEM* **1989**, *187*, 271–283.

[17] P. Tarakeshwar and S. Manogaran, An *ab initio* study of pyruvic acid, *J. Mol. Struct.: THEOCHEM* **1998**, *430*, 51–56.

[18] Z. Y. Zhou, D. M. Du, and A. P. Fu, Structures and vibrational frequencies of pyruvic acid: Density functional theory study, *Vibr. Spectr.* **2000**, *23*, 181–186.

[19] R. Fausto, L. A. E. Batista de Carvalho, and J. J. C. Teixeira–Dias, Molecular structure and properties of thoacetic acid, *J. Mol. Struct.: THEOCHEM* **1990**, *207*, 67–83.

[20] D. W. Liao, A. M. Mebel, M. Hayashi, Y. J. Shiu, Y. T. Chen, and S. H. Lin, *Ab initio* study of the n–π* electronic transition in acetone: Symmetry–forbidden vibronic spectra, *J. Chem. Phys.* **1999**, *111*, 205–215.

[21] K. –M. Marstokk and H. Møllendal, Microwave spectrum, conformation, barrier to internal rotation and dipole moment of pyruvic acid, *J. Mol. Struct*, **1974**, *20*, 257–267.

[22] C. E. Dyllick–Brenzinger, A. Bauder, and Hs. H. Günthard, The substitution, structure, barrier to internal rotaion, and low frequency vibrations of pyruvic acid, *Chem. Phys.* **1977**, *23*, 195–206.

[23] R. Meyer and A. Bauder, Torsional coupling in pyruvic acid, *J. Mol. Spectrosc.* **1982**, *94*, 136–149.

[24] W. J. Ray, J. E. Katon, and D. B. Philips, Structure, hydrogen bonding and vibrational spectra of pyruvic acid, *J. Mol. Struct.* **1981**, *74*, 75–84.

[25] M. S. Gordon and D. E. Tallman, Localized orbital studies of hydrogen bonding. General approach and applications to water, formic acid, and pyruvic acid, *Chem. Phys. Lett.* **1972**, *17*, 385–392.

[26] K. Saito, G. Sasaki, and S. Tanaka, Unimolecular decomposition of pyruvic acid: an experimental and theoretical study, *J. Phys. Chem.* **1994**, *98*, 3756–3761.

[27] C. Wesdemiotis and F. W. McLafferty, Hydroxyethylidene ($CH_3$–C–OH), but not ethenol, tautomerizes to ethanol, *J. Am. Chem. Soc*, **1987**, *109*, 4760–4761.

[28] K. E. Norris, G. B. Bacskay and J. E. Gready, Theoretical study of "Protonated Pyruvate": A methylhydroxycarbene–carbon dioxide complex– Implications for the decarboxylation of pyruvic acid, *J. Comput. Chem.* **1993**, *14*, 699–714.

[29] J. L. Holmes and F. P. Lossing, Heats of formation of the ionic and neutral enols of acetaldehyde and acetone, *J. Am. Chem. Soc.* **1982**, *104*, 2648–2649.

[30] B. J. Smith, M. T. Nguyen, W. J. Bouma and L. Radom, Unimolecular rearrangements connecting hydroxyethylidene ($CH_3$–C–OH), acetaldehyde ($CH_3$–CH:O), and vinyl alcohol ($CH_2$:CH–OH), *J. Am. Chem. Soc.*, **1991**, *113*, 6452–6458.

[31] J. F. Liebman and J. Simons, In *Molecular Structure and Energetics. Volume 1. Chemical Bonding Models*, J. F. Liebman and A. Greenberg, Eds., VCH Publishers, Deerfield Beach, FL, **1986**, p. 51.

[32] J. S. Yadav and J. D. Goddard, Methoxycarbene and methylhydroxycarbene: energies, structures, vibrational frequencies, and unimolecular reactivities, *J. Chem. Phys.* **1986**, *85*, 3975–3984.

[33] J. D. Evanseck and K. N. Houk, Theoretical predictions of activation energies for 1,2–hydrogen shifts in singlet carbenes, *J. Phys. Chem.* **1990**, *94*, 5518–5523.

[34] M. Räsänen, T. Raaska, H. Kunttu, and J. Murto, *Ab initio* studies on carbenes; singlet and triplet conformers and vibrational spectra of hydroxy–, dihydroxy– and methylhydroxy–carbene, *J. Mol. Struct. THEOCHEM* **1990**, *208*, 79–90.

[35] R. A. Poirier, D. Majlessi, and T. J. Zielinski, An SCF and CI study of the 1,3 shift in the HX–CH=Y ↔ X=CH–YH isolectronic series: X, Y = $CH_2$, NH and O, *J. Comput. Chem.* **1986**, *7*, 464–475.

## Biographies

**Rita Kakkar** is a Professor of Chemistry at the University of Delhi, India. After obtaining a Ph.D. degree in Physical Chemistry from the University of Delhi, Dr. Rita Kakkar undertook postdoctoral research on various topics related to computational chemistry. She has successfully supervised 13 Ph. D. theses, and has been teaching physical chemistry at the University of Delhi for the past 20 years. Her major interests are theoretical modeling of reaction paths, including biochemical pathways, calculating rate constants and isotope effects using quantum statistical approaches, and determination of equilibrium structures of tautomeric systems, especially in relation to biological systems. More recently, she has started research on density functional studies on adsorption and dissociation on nanosurfaces. This research has applications in pollution control, as the information obtained in these studies can help design better adsorbents for controlling air quality, particularly indoor air. Prof. Rita Kakkar has 47 research publications in journals of international reputation.

**Preeti Chadha** is presently a Lecturer of Physical Chemistry at Sri Venkateswara College, University of Delhi. She has recently completed her Ph. D. under Professor Rita Kakkar's supervision. The title of her thesis is "Density Functional Studies of Carbene Rearrangements".

**Deepshikha Verma** undertook this research in partial fulfillment of the requirements for the M. Phil. degree of the University of Delhi. She is presently employed at the National Thermal Power Corporation (NTPC), a Government of India undertaking.